able CD21 on B cells without diminishing their expression of CD19.

Mice were co-immunized subcutaneously in PBS with 25 μg of keyhole limpet hemocyanin (KLH) alone or in the presence of 0.5 pmol of HEL-C3d_3. The IgG1 response to KLH on day 14 was not altered by HEL-C3d_3, which indicates that C3d modifies the response only to the antigen to which it is bound.

These findings demonstrate that the immunity-augmenting function of the complement system is mediated solely by a discrete molecular modification of antigen, attachment of C3d, and that the magnitude of enhancement may be as great as 10,000-fold, which is far greater than even that of CFA. Three mechanisms may mediate this function. First, the association of CD21 with CD19, which is tyrosine-phosphorylated when mIg is ligated and binds phosphatidylinositol-3 kinase (*15*) and Vav (*16*), links the complement receptor to cytosolic effectors of signaling that amplify activation of B cells. The important role of CD19 in the humoral immune response recently has been exemplified in mice lacking this B cell protein (*4*). Second, the avidity with which low-affinity, unprimed B cells bind antigen is probably enhanced by the interaction of CD21 with C3d. Third, CD21 is expressed on follicular dendritic cells that may promote the development and maintenance of memory B cells (*17*).

The complement system, through the adjuvant effect of C3d, may select antigens for recognition by the acquired immune system. This function would be complementary to that of other components of innate immunity, such as macrophages, natural killer cells, and mast cells, which produce cytokines that may determine the character of an acquired immune response by directing the development of T helper type 1 and type 2 cells. Together, these humoral and cellular elements enable the acquired immune system to respond appropriately to potentially noxious foreign antigens. Their manipulation may lead to more effective strategies for vaccination.

REFERENCES AND NOTES

1. C. A. Janeway Jr., *Immunol. Today* **13**, 11 (1992); P. Matzinger, *Annu. Rev. Immunol.* **12**, 991 (1994).
2. D. T. Fearon and K. F. Austen, *N. Engl. J. Med.* **303**, 259 (1980); H. J. Müller-Eberhard, *Annu. Rev. Biochem.* **57**, 321 (1988).
3. D. T. Fearon and R. H. Carter, *Annu. Rev. Immunol.* **13**, 127 (1995); T. F. Tedder, L. J. Zhou, P. Engel, *Immunol. Today* **15**, 437 (1994).
4. R. C. Rickert, K. Rajewsky, J. Roes, *Nature* **376**, 352 (1995); P. Engel *et al.*, *Immunity* **3**, 39 (1995).
5. M. B. Pepys, *J. Exp. Med.* **140**, 126 (1974); B. Heyman, E. J. Wiersma, T. Kinoshita, *ibid.* **172**, 665 (1990).
6. T. Hebell, J. M. Ahearn, D. T. Fearon, *Science* **254**, 102 (1991).
7. The complementary DNA encoding HEL, C3d [H. Domdey *et al.*, *Proc. Natl. Acad. Sci. U.S.A.* **79**, 7619 (1982)], dog pre-pro-insulin signal sequence [M. E. Taylor and K. Drickamer, *Biochem. J.* **274**, 575 (1991)], and the $(G_4S)_2$ linker were amplified by polymerase chain reaction. The epitope tag and stop codon were coded for by oligonucleotide linkers. Fusion protein cassettes were assembled in tandem: dog pre-pro-insulin signal sequence, HEL, and one to three copies of C3d linked by $(G_4S)_2$ in pSG5 (Stratagene). The HEL-C3d_3 cassette was subcloned into the A71d vector. The plasmids pSG.HEL, pSG.HEL.C3d, and pSG.HEL.C3d_2 were co-transfected with pSV2-neo into L cells, and A71d. HEL.C3d_3 was transiently expressed in COS cells. Recombinant proteins were purified by affinity chromatography on YL 1/2 antibody [R. H. Skinner *et al.*, *J. Biol. Chem.* **266**, 14163 (1991)] and fractionation on Sephacryl S-200 (Pharmacia).
8. S. J. Smith-Gill *et al.*, *J. Immunol.* **128**, 314 (1981).
9. The anti-HEL mIgM-IgD transgenic mice MD4 (*18*) were maintained on a C57BL/6 background. The F_1 mice were produced by crossing MD4 with CBA/Ca (Harlan, Bicester, UK). Animal experiments were done according to procedures regulated under the Project License issued by the U.K. Home Office.
10. Raji cells, 3×10^7 to 4×10^7 cells/ml, were incubated for 45 min at 4°C with 1 nM [^{125}I]HEL-C3d_2 (specific activity, 9.1×10^5 cpm/μg) and incremental concentrations of the HEL-C3d fusion proteins, 500 nM $(CR2)_2$-IgG1 (*6*), or IgG1 in PBS containing 0.1% bovine serum albumin. The cells were centrifuged through a dibutyl-diiso-octyl pthalate cushion, and the amount of ^{125}I bound to the cell pellet was determined.
11. Transgenic and nontransgenic splenocytes, 6×10^6 cells/ml in 10% fetal calf serum + RPMI + 50 μM 2-mercaptoethanol, were loaded with 2 μM indo 1-AM, washed, and stained with 10 μg/ml of phycoerythrin (PE)-conjugated anti-CD43 (Pharmingen). Changes in $[Ca^{2+}]_i$ were monitored by flow cytometric analysis (FACStar, Becton Dickinson) of PE-negative cells after addition of incremental concentrations of recombinant proteins.
12. T. Kinoshita *et al.*, *J. Immunol.* **140**, 3066 (1988).
13. All mice were 4- to 8-week-old CBA/Ca males purchased from Harlan. Recombinant antigens were diluted in PBS containing 0.1% globulin-free murine albumin (Sigma) and administered in this buffer alone or after emulsification with equal volumes of IFA or CFA. Primary immunizations of 0.1 ml were administered subcutaneously to the right rear flank. Secondary immunizations of 0.1 ml in IFA were administered intraperitoneally. HEL-specific IgG1 was assayed by enzyme-linked immunosorbent assay (ELISA) (*18*) using horseradish peroxidase–conjugated goat antibody to mouse IgG1 (Southern Biotechnology Associates) and microtiter plates coated with HEL (Sigma). Use of recombinant HEL and HEL-C3$d_{1\text{-}3}$ as antigens in the ELISA gave comparable results. The data are represented as mean relative units (RU) + 1 SD based on a standard curve established with pooled sera from hyperimmunized mice.
14. 1D3 is a rat monoclonal IgG2a antibody to mouse CD19 (I. Krop *et al.*, *Eur. J. Immunol.*, in press). For fluorescence-activated cell sorting analysis, splenocytes were stained with 5 μg/ml of 7G6, 1D3, or control antibody followed by PE-conjugated goat antibody to rat F(ab)$_2$ (CalTag).
15. D. A. Tuveson, R. H. Carter, S. P. Soltoff, D. T. Fearon, *Science* **260**, 986 (1993).
16. W.-K. Weng, L. Jarvis, T. W. LeBien, *J. Biol. Chem.* **269**, 32514 (1994).
17. I. C. M. MacLennan, *Annu. Rev. Immunol.* **12**, 117 (1994).
18. C. C. Goodnow *et al.*, *Nature* **334**, 676 (1988).

19. We thank G. Fey for the murine C3 complementary DNA, K. Drickamer for the dog pre-pro-insulin signal sequence, R. Smith for help in producing recombinant proteins, A. Venkitaraman for the A71d vector, and C. Milstein for the YL 1/2 antibody. Supported by the Wellcome Trust (D.T.F. and P.W.D.), NIH grant AI07247 (P.W.D.), and the Medical Research Council (M.E.D.A.), Howard Hughes Medical Institute (S.A. and C.C.G.), and NIH grant AI19512 (C.C.G.).

14 September 1995; accepted 23 November 1995

DPC4, A Candidate Tumor Suppressor Gene at Human Chromosome 18q21.1

Stephan A. Hahn, Mieke Schutte, A. T. M. Shamsul Hoque, Christopher A. Moskaluk, Luis T. da Costa, Ester Rozenblum, Craig L. Weinstein, Aryeh Fischer, Charles J. Yeo, Ralph H. Hruban, Scott E. Kern*

About 90 percent of human pancreatic carcinomas show allelic loss at chromosome 18q. To identify candidate tumor suppressor genes on 18q, a panel of pancreatic carcinomas were analyzed for convergent sites of homozygous deletion. Twenty-five of 84 tumors had homozygous deletions at 18q21.1, a site that excludes *DCC* (a candidate suppressor gene for colorectal cancer) and includes *DPC4*, a gene similar in sequence to a *Drosophila melanogaster* gene (*Mad*) implicated in a transforming growth factor–β (TGF-β)–like signaling pathway. Potentially inactivating mutations in *DPC4* were identified in six of 27 pancreatic carcinomas that did not have homozygous deletions at 18q21.1. These results identify *DPC4* as a candidate tumor suppressor gene whose inactivation may play a role in pancreatic and possibly other human cancers.

The development of human cancer involves the clonal evolution of cell populations that gain competitive advantage over other cells through the alteration of at least two distinct classes of genes: proto-oncogenes and tumor suppressor genes (*1*). Tumor suppressor genes are characterized by alterations that inactivate both alleles (*2*). Many tumor suppressor genes are inactivated by intragenic mutations in one allele accompanied by the loss of a chromosomal region containing the other allele, termed loss of heterozygosity (LOH). Mapping of homozygous deletions within regions showing a high frequency of LOH has been a critical step in the discovery of several tumor suppressor genes (*3*).

Human pancreatic ductal carcinomas

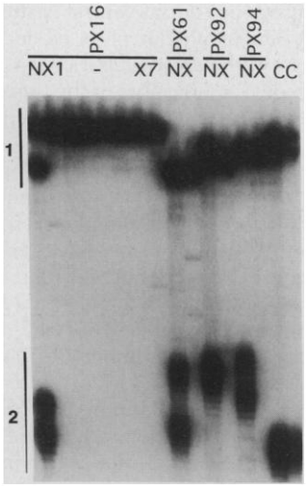

Fig. 1. Homozygous deletions of chromosome 18q21.1 in four pancreatic carcinoma xenografts, as identified by multiplex PCR. The smaller products (migrating in size range 2, marked at left) were produced by microsatellite marker D18S46. The larger products (size range 1) represent internal positive controls from a retained microsatellite locus (D18S68) outside the deleted region. Tumor PX16 is represented by seven parallel xenografts, independently derived from the same primary tumor tissue. N, normal DNA, X, xenograft DNA, C, control (normal human DNA).

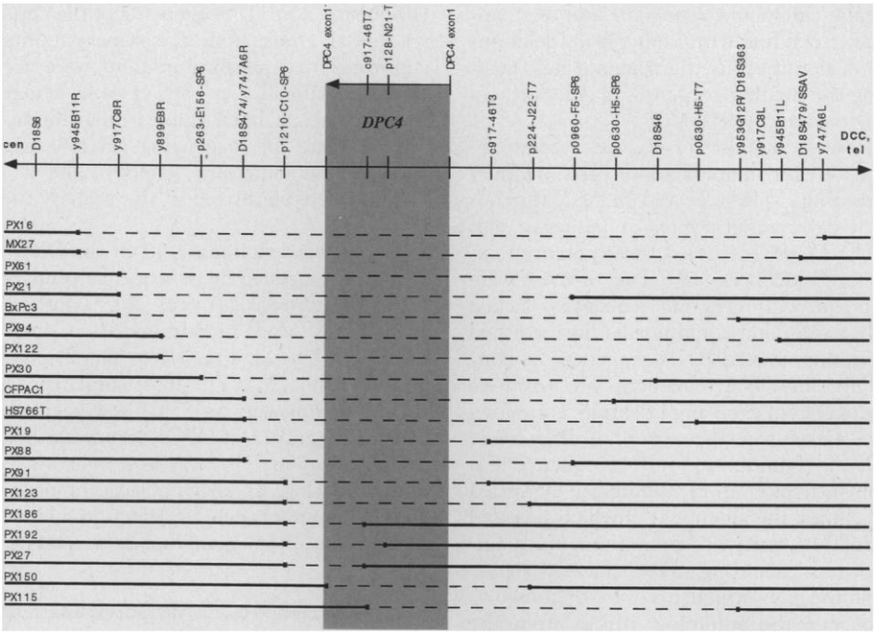

Fig. 2. Regional map of the homozygous deletions on 18q. Markers are arbitrarily spaced, to reflect relative positions. The shaded area represents the coding region of the *DPC4* gene. Prefix "y" indicates YAC-derived markers; "p," P1-PAC markers; and "c," cosmid markers. The solid lines for each cancer represent the areas without homozygous deletion (when all markers in the region were present), and the broken lines represent the areas of homozygous deletion. All specimens designated with PX are pancreatic carcinoma xenografts, except for PX115, which is a biliary carcinoma xenograft. MX27 is a xenograft derived from a bladder carcinoma. BxPc3, CFPAC1, and HS766T are pancreatic carcinoma cell lines; cen, direction to centromere; tel, to telomere.

display consistent genetic changes, including Ki-*ras* mutations (>80%) (*4*, *5*), *p53* mutations (50 to 70%) (*5*), and p16 mutations or homozygous deletions (>85%) (*6*). Allelotype data suggest the existence of additional tumor suppressor genes at other loci (*7*), most notably on chromosome 18q, which shows LOH in nearly 90% of pancreatic cancers (*7*). A candidate suppressor gene for colorectal cancer, *DCC* (deleted in colorectal carcinoma), is located on 18q, but because of the length and complexity of the gene (29 exons spanning 1.4 megabases), its mutational status in pancreatic and other carcinomas is unknown (*8*).

We searched for deletions that would potentially localize tumor suppressor genes on chromosome 18 by performing a genome scan with 11 spaced polymerase chain reaction (PCR)–based markers. A consensus deletion site could not be established from the LOH pattern because the deletions often spanned most of the chromosomal arm (*9*). However, four of 31 xenografts of pancreatic carcinoma had a homozygous deletion involving two contiguous loci (defined by microsatellite markers D18S46 and D18S363) centromeric to *DCC* (*10*). Multiple sequence-tagged site (STS) markers within or flanking the *DCC* gene showed that the deletions did not include *DCC*. These results were confirmed in repeated PCRs, in multiplex PCRs, and in several parallel xenografts derived independently from the original primary carcinomas (Fig. 1) (*11*). Southern (DNA) blot analysis, performed on three of these four cancers, revealed that the markers were absent from tumor DNA samples, but present in constitutional DNA samples from the same patients, confirming the homozygous deletions (*11*).

Markers D18S46 and D18S363 were used to screen the CEPH (Centre d'Etudes du Polymorphisme Humaine) mega-YAC (yeast artificial chromosome) library by PCR (*12*). Seven YAC clones were identified, and in turn two additional overlapping YAC clones were found within the on-line hybridization data of the CEPH database. STS markers were derived from isolated YAC ends and used to build a YAC contig (*13*). A tumor panel consisting of 41 xenografts derived from primary pancreatic adenocarcinomas, 10 pancreatic cell lines, 22 breast cancer cell lines, and xenografts of four primary biliary cancers and two primary bladder cancers, were screened with STS markers derived from the YAC ends and from known markers within the contig. An additional 10 homozygous deletions were identified within this tumor panel (six in the pancreatic xenografts, two in pancreatic cell lines, one in the bladder, and one in the biliary cancer) (Fig. 2). Two of 178 colorectal cancer cell lines and xenografts were also found to harbor a homozygous deletion upon screening with these STS markers (*14*).

The smallest consensus of deletion was defined by STS markers y747A6R and D18S474 on the centromeric end and D18S46 on the telomeric end. None of the deletions extended beyond YAC-end y747A6L, the telomeric border of the contig. YAC y747A6 also contains the SSAV locus, located approximately 2 megabases centromeric to *DCC* (*15*). Starting from markers D18S46 and D18S474, we performed P1 and P1 artificial chromosome (PAC) library screens, which yielded a contig spanning the consensus region of deletion (*16*). Three YACs, which together spanned the consensus of deletion, were subcloned into a cosmid vector. Cosmids were integrated into the P1-PAC contig, and end sequences from P1s, PACs, and selected cosmids were used to define new STS markers (*17*). An additional three pan-

S. A. Hahn, M. Schutte, A. T. M. S. Hoque, C. A. Moskaluk, E. Rozenblum, C. L. Weinstein, A. Fischer, R. H. Hruban, Department of Pathology, Johns Hopkins University School of Medicine, Baltimore, MD 21205, USA.
L. T. da Costa, Graduate Program in Human Genetics and Molecular Biology, Johns Hopkins University School of Medicine, Baltimore, MD 21205, USA.
C. J. Yeo, Department of Surgery, Johns Hopkins University School of Medicine, Baltimore, MD 21205, USA.
S. E. Kern, Department of Oncology, Johns Hopkins University School of Medicine, Baltimore, MD 21205, USA.
*To whom correspondence should be addressed.

creatic carcinoma xenografts and one pancreatic cell line with homozygous deletions were identified in the tumor panel, mapping the smallest consensus of deletion to a single cosmid (c917-46).

Using cosmid c917-46, and a combination of exon amplification, cDNA library screening, 5′-RACE, and BLAST searches of a database of expressed sequence tags (dbEST), we identified three potential expressed sequences (*18*). Two of these were colinear with genomic sequences, lacked splice sites, and could not be distinguished from unprocessed RNA sequences or contaminating DNA sequences. The third sequence, from exon amplification, contained a 51–base pair (bp) open reading frame (ORF). Hybridization of this sequence to a human fetal brain cDNA library identified 19 clones, the alignment of which revealed a 2680-bp transcript from a previously unreported gene (Fig. 3). Primers designed from the cDNA sequence were then used to sequence the adjoining introns from the genomic clones (c917-46 and p128-N21). The predicted 552 amino acid coding sequence of this gene was defined by (i) multiple stop codons in all three reading frames 5′ to the putative ATG start site; (ii) multiple stop codons in the noncoding frames 3′ to the start site; (iii) 10 splice sites (11 exons) in the longest possible ORF; and (iv) a terminal TGA stop codon in-frame, as well as stop codons nearby in the other two frames. We designated the gene *DPC4* [for homozygously deleted in pancreatic carcinoma, locus 4, following the order of previously described loci (*6*, *7*)].

Analysis of 61 pancreatic xenografts (*19*) with four expressed sequence tags (ESTs) derived from the coding region of *DPC4* revealed nine new homozygous deletions, five with endpoints within *DPC4*. Thus, this gene was homozygously deleted in a total of 25 (30%) of 84 pancreatic carcinomas. Further screening of 14 xenografts by an in vitro–synthesized protein assay identified one (PX101) that expressed a truncated protein suggestive of an intragenic point mutation (*20*). For all 14 cancers, the reverse transcriptase (RT)–PCR product length matched the predicted size of the full-length transcript.

Genomic sequencing of all 11 *DPC4* exons was performed for 27 pancreatic xenografts that did not have a homozygous deletion of the gene (*21*). Six mutations were identified (Table 1), including a mutation creating a nonsense codon in exon 11 (PX101, confirming the protein assay result), a nonsense mutation in exon 8 (PX23) and in exon 9 (PX74), a splice donor site mutation after exon 10 (PX28), an 8-bp frameshift microdeletion (PX102), and a missense mutation producing a nonconservative amino acid substitution (PX86) in exon 11. Sequencing of the constitutional DNA from the same patients confirmed that all six mutations were acquired somatically. In both cases in which the surgical specimen yielded tumor material adequate for sequencing (PX101 and PX102), the mutations found in the xenografts were confirmed in the primary tumors (*22*).

A possible functional role for the DPC4 protein is suggested by its sequence similarity to the *Drosophila melanogaster* Mothers against dpp (Mad) protein and the *Caenorhabditis elegans* Mad homologs sma-2, sma-3, and sma-4 (*23*). The most similarity to these proteins (up to 85%) was seen in exons 1, 2, and 11 of *DPC4*; somewhat less similarity (up to 75%) was seen in exons 8, 9, and 10 (Fig. 4). In *Drosophila*, homozygous Mad mutants exhibit defects in midgut morphogenesis, imaginal disc development, and embryonic dorsal-ventral patterning (*23*). A similar phenotype is produced by mutations in the *decapentaplegic* (*dpp*) gene, which codes for a member of the transforming growth factor–β (TGF-β) superfamily and appears to play a central role in intercellular signaling throughout development (*24*). It is noteworthy that a stop mutation responsible for the Mad phenotype, located at codon 417 within a conserved region of the *Mad* gene, matches the position of the frameshift mutation found in *DPC4* (PX102) and is located one codon 5′ to the position of a nonsense mutation found in *DPC4* (PX101) (Table 1) (*23*).

TGF-β is a potent inhibitor of cellular proliferation for most normal cells (*24*), and many cancer cells show diminished responsiveness to TGF-β–induced growth inhibition. This may be due to inactivation of cell cycle regulatory proteins that mediate

```
  1  MDNMSITNTPTSNDACLSIVHSLMCHRQGGESETFAKRAIESLVKKLKEKKDELDSLITAITTNGAHPSKCVTIQRTLDG  80
 81  RLQVAGRKGFPHVIYARLWRWPDLHKNELKHVKYCQYAFDLKCDSVCVNPYHYERVVSPGIDLSGLTLQSNAPSSMMVKD 160
161  EYVHDFEGQPSLSTEGHSIQTIQHPPSNRASTETYSTPALLAPSESNATSTANFPNIPVASTSQPASILGGSHSEGLLQI 240
241  ASGPQPGQQQNGFTGQPATYHHNSTTTWTGSRTAPYTPNLPHHQNGHLQHHPPMPPHPGHYWPVHNELAFQPPISNHPAP 320
321  EYWCSIAYFEMDVQVGETFKVPSSCPIVTVDGYVDPSGGDRFCLGQLSNVHRTEAIERARLHIGKGVQLECKGEGDVWVR 400
401  CLSDHAVFVQSYYLDREAGRAPGDAVHKIYPSAYIKVFDLRQCHRQMQQQAATAQAAAAAQAAAVAGNIPGPGSVGGIAP 480
485  AISLSAAAGIGVDDLRRLCILRMSFVKGWGPDYPRQSIKETPCWIEIHLHRALQLLDEVLHTMPIADPQPLD 552
```

Fig. 3. Predicted amino acid sequence of the *DPC4* gene product. The nucleotide sequence has been deposited in GenBank (accession number U44378). Abbreviations for the amino acid residues are A, Ala; C, Cys; D, Asp; E, Glu; F, Phe; G, Gly; H, His; I, Ile; K, Lys; L, Leu; M, Met; N, Asn; P, Pro; Q, Gln; R, Arg; S, Ser; T, Thr; V, Val; W, Trp; and Y, Tyr.

Table 1. *DPC4* sequence changes in pancreatic carcinomas.

Specimen	Codon	Mutation	Predicted effect
PX23	358	GGA to TGA	Gly to Stop
PX74	412	TAC to TAG	Tyr to Stop
PX28	483	AGT to AAT	Aberrant splicing
PX86	493	GAT to CAT	Asp to His
PX101	515	AGA to TGA	Arg to Stop
PX102	516–518	CAGAGCATC to C	Frameshift

```
DPC4   27  RQGGESETFAKRAIESLVKKLKEKKDELDSLITAITTNGAHPSKCVTIQRTLDGRLQV
sma2   17  KQGDEDENWAKKAIDNLMKKL---KQALENLEFALRCQGQQKTECVTIPRSLDGRLQI
Mad    35  KQGDEEEKWAEKAVDSLVKKLKKRKGAIEELERALSCPGQ-PSKCVTIPRSLDGRLQV

DPC4   85  AGRKGFPHVIYARLWRWPDLHKNELKHVKYCQYAFDLKCDSVCVNPYHYERVVSPGI
sma2   92  SHRKALPHVIYCRVYRWPDL--HELKAIEDCRFCYESGQKDICINPYHYKRVHATGV
Mad    76  SHRKGLPHVIYCRVWRWPDL--HELKPLELCQYPFSAKQKEVCINPYHYKRVESPVL

DPC4  316  NHPAPEYWCSIAYFEMDVQVGETFKVPSSCPIVTVDGYVDPSGGDRFC
sma2  215  KVWEEQFWATVSYYELNTRVGEQVKVSST---ITIDGFTDPCINGSKI
Mad   254  SYSEPAFWASIAYYELNCRVGEVFHCNNNS--VIVDGFTNPSNNSDRC

DPC4  357  SGGDRFCLGQLSNVHRTEAIERARLHIGKGVQLECKGEGDVWVRCLSDHAVFVQS
sma2  255  INGSKISLGLFSNVNRNATIENTRRHIGNGVKL--RSNGSLFAQCESDSAIFVQS
Mad   294  NNSDRCCLGQLSNVNRNSTIENTRRHIGKGVHL-----GE YAECLSDSAIFVQS

DPC4  492  VDDLRRLCILRMSFVKGWGPDYPRQSIKETPCWIEIHLHRAL LLDEVLHTM
sma2  356  SFDLQKMTFIRMSFVKGWGAEYQRQDVTSTPCWIEIHLHAPLAWLDRVLSTM
Mad   393  VYELTKMCTIRMSFVKGWGAEYHRQDVTSTPCWIEIHLHGPL WLDKVLTQM
```

Fig. 4. Amino acid sequence similarities between human DPC4, *D. melanogaster* Mad, and *C. elegans* sma-2. Amino acid identities are in black; conservative changes are in gray. Gaps introduced for maximal alignment are marked with dashes. Numbers indicate codon positions at which individual alignments begin.

this response (25) or to mutations in TGF-β receptors (26). Transfer of chromosome 18 has been shown to partially restore TGF-β responsiveness to a cancer cell line (27), consistent with the notion that this chromosome carries a gene involved in TGF-β–induced growth suppression. The relationship of the signaling pathways initiated by TGF-β and other members of the TGF-β superfamily, however, is unclear. Studies of the *DPC4* pathway and its association with members of the TGF-β superfamily in pancreatic carcinoma and other model systems should be instructive for the further understanding of the role of *DPC4* in human neoplasia.

REFERENCES AND NOTES

1. R. A. Weinberg, *Science* **254**, 1138 (1991); J. M. Bishop, *ibid.* **235**, 305 (1987).
2. A. G. Knudson Jr., *Cancer Res.* **45**, 1437 (1985).
3. T. P. Dryja, J. M. Rapaport, J. M. Joyce, R. A. Petersen, *Proc. Natl. Acad. Sci. U.S.A.* **83**, 7391 (1986); E. R. Fearon *et al.*, *Science* **247**, 49 (1990); A. Kamb *et al.*, *ibid.* **264**, 436 (1994).
4. C. Almoguerra *et al.*, *Cell* **53**, 549 (1988); R. H. Hruban *et al.*, *Am. J. Pathol.* **143**, 545 (1993).
5. M. S. Redston *et al.*, *Cancer Res.* **54**, 3025 (1994).
6. C. Caldas *et al.*, *Nature Genet.* **8**, 27 (1994).
7. S. A. Hahn *et al.*, *Cancer Res.* **55**, 4670 (1995).
8. K. R. Cho *et al.*, *Genomics* **19**, 525 (1994).
9. S. A. Hahn, A. T. M. Shamsul Hoque, S. E. Kern, unpublished data.
10. Data on microsatellite markers, and the corresponding primer sequences, were accessed through the Cooperative Human Linkage Center (http://www.chlc.org/HomePage.html) or from the Human Genome Database (http://gdbwww.gdb.org/).
11. The methods for establishing xenografts and for PCR and multiplex PCR assays were as in (7), and for Southern blots as in (6). STS markers used to exclude the involvement of *DCC* were SSAV, D18S523, D18S526, D18S101, and the microsatellite marker *DCC* (15). All PCR reactions were repeated at least three times and confirmed by a second primer pair designed on nearby sequences to exclude the possibility of a primer site polymorphism. The quality of the DNA was further ensured by the successful amplification of a 1.8-kb fragment (exons 5 to 9 of p53) and of numerous primer sets for microsatellite markers.
12. D. Cone, I. Chumakow, J. Weissenbach, *Nature* **366**, 698 (1993).
13. YAC ends were isolated by the inverse PCR technique (28). The amplified ligation fragments were sequenced by cycle sequencing (SequiTerm, Epicentre Technologies, Madison), and 20-mer oligonucleotide pairs for STS markers were designed. PCR analysis of monochromosomal somatic cell hybrid DNA (NIGMS mapping panel 2, Coriell Cell Repositories) confirmed STS localization to chromosome 18. The full genomic map is published [S. A. Hahn *et al.*, *Cancer Res.*, in press].
14. F. S. Leach and B. Vogelstein, personal communication.
15. U. Francke *et al.*, *Cytogenet. Cell Genet.* **66**, 196 (1994).
16. A PCR-based P1 screening was performed by Genome Systems, St. Louis, with STS markers flanking the consensus deletion. Positive P1 clones from the DuPont Merck Pharmaceutical Company Human Foreskin Fibroblast Library 1 (DMPC-HFF#1) were: 1210-C10, 0960-F5, and 0630-H5. We performed a second screen with human PAC library (purchased from Genome Systems) by hybridizing a random primer-labeled PCR product to gridded PAC library filters.
17. Partial Nde II–digested YAC DNA was subcloned into the SuperCos-I vector (Stratagene). Cosmids were screened and identified by PCR with STS markers derived from the region of interest and were sequenced using primers specific for vector sequences. P1-PAC end sequences were generated by direct sequencing or by a PCR-based amplification technique [Y.-G. Liu, R. F. Whittier, *Genomics* **25**, 674 (1995) and L. T. da Costa, unpublished data].
18. For exon amplification, DNA from cosmid c917-46 was digested with Bam HI and Bgl II and ligated into the pSPL3 exon-trapping vector (Gibco/BRL). Exon-trapped sequences were analyzed by BLAST homology searches. The location of the exon-trapped sequences to the region was confirmed by Southern blot analysis of Eco RI–digested DNA of cosmid c917-46. 5′-RACE was performed according to the manufacturer's instructions (Clontech, Palo Alto). cDNA library screening was performed with exon-trapped sequences or Eco RI restriction fragments from c917-46 as probes. The cDNA libraries were derived from HeLa cells, human placenta, and human fetal brain (Stratagene), and the human colorectal cancer cell line SW480 (Clontech).
19. These 61 xenografts included 28 from the initial panel and 33 new ones.
20. The protein assay was performed with the TNT kit (Promega). Primer sequences (5′ to 3′) were: DPC4S, GGATCCTAATACGACTCACTATAGGGCCGCCACCATGGCCTGTCTGAGCATTGTGCATAG; and DPC4AS, CAGTTTCTGTCTGCTAGGAG [M. W. Powell *et al.*, *N. Engl. J. Med.* **329**, 1982 (1993)].
21. PCR amplification of the exons was performed as in (29). Mutations were confirmed in a second PCR reaction. The PCR primer sequences are available upon request. Intronic primers were generally used to amplify exons from the xenografts grown in mice, because exonic primers generated PCR products from mouse DNA that were identical in size to the human PCR products.
22. Direct sequencing of microdissected tumor cells was achieved in two of the six tumors with *DPC4* mutations. Contamination of normal cells in primary pancreatic carcinomas usually precludes direct genetic study (7).
23. J. J. Sekelsky, S. J. Newfeld, L. A. Raftery, E. H. Chartoff, W. M. Gelbart, *Genetics* **139**, 1347 (1995).
24. D. A. Hursh, R. W. Padgett, W. M. Gelbart, *Development* **117**, 1211 (1993).
25. M. G. Alexandrow and H. Moses, *Cancer Res.* **55**, 1452 (1995); G. J. Hannon and D. Beach, *Nature* **371**, 257 (1994).
26. S. Markowitz *et al.*, *Science* **268**, 1336 (1995).
27. M. C. Goyette *et al.*, *Mol. Cell. Biol.* **12**, 1387 (1992).
28. G. A. Silverman, *PCR Methods Applic.* **3**, 141 (1993).
29. M. Schutte *et al.*, *Proc. Natl. Acad. Sci. U.S.A.* **92**, 5950 (1995).

30. We thank K. W. Kinzler and B. Vogelstein for cDNA library clones. Supported by the SPORE in Gastrointestinal Cancer, NIH grant CA62924, Deutsche Krebshilfe (S.A.H.), and Junta Nacional de Investigação Científica e Technológica Scholarship BD1508/91 (L.T.C.). S.K. is a McDonnell Foundation Scholar.

16 November 1995; accepted 18 December 1995

rad-Dependent Response of the *chk1*-Encoded Protein Kinase at the DNA Damage Checkpoint

Nancy C. Walworth* and Rene Bernards

Exposure of eukaryotic cells to agents that generate DNA damage results in transient arrest of progression through the cell cycle. In fission yeast, the DNA damage checkpoint associated with cell cycle arrest before mitosis requires the protein kinase $p56^{chk1}$. DNA damage induced by ultraviolet light, gamma radiation, or a DNA-alkylating agent has now been shown to result in phosphorylation of $p56^{chk1}$. This phosphorylation decreased the mobility of $p56^{chk1}$ on SDS–polyacrylamide gel electrophoresis and was abolished by a mutation in the $p56^{chk1}$ catalytic domain, suggesting that it might represent autophosphorylation. Phosphorylation of $p56^{chk1}$ did not occur when other checkpoint genes were inactive. Thus, $p56^{chk1}$ appears to function downstream of several of the known *Schizosaccharomyces pombe* checkpoint gene products, including that encoded by $rad3^{+}$, a gene with sequence similarity to the *ATM* gene mutated in patients with ataxia telangiectasia. The phosphorylation of $p56^{chk1}$ provides an assayable biochemical response to activation of the DNA damage checkpoint in the G_2 phase of the cell cycle.

Proliferating eukaryotic cells arrest progression through the cell cycle in response to DNA damage (1). Failure to repair damaged DNA can result in the propagation of mutations or damaged chromosomes and, therefore, may contribute to genetic instability and cancer (2, 3). The mechanism responsible for monitoring the integrity of the genome and preventing progression through the cell cycle in the event of DNA damage has been described as the DNA damage checkpoint (3). The signal transduction pathway that couples detection of DNA damage to control of progression through the cell cycle has yet to be elucidated. Several radiation-sensitive mutants (*rad* mutants) of both the budding yeast *Saccharomyces cerevisiae* and the fission yeast *Schizosaccharomyces pombe* have been identified (3–8). These mutants define components of the checkpoint pathway because they are unable to arrest the cell cycle when DNA is damaged (3–8).

When present in multiple copies per cell, the *chk1*-encoded protein kinase (6) can suppress the growth defect associated with particular mutant alleles of the gene that encodes $p34^{cdc2}$, a highly conserved cyclin-dependent kinase that governs cell

Division of Molecular Carcinogenesis, Netherlands Cancer Institute, Plesmanlaan 121, 1066 CX Amsterdam, Netherlands.

*To whom correspondence should be directed at present address: Department of Pharmacology, UMDNJ–Robert Wood Johnson Medical School, 675 Hoes Lane, Piscataway, NJ 08854-5635, USA.